ELECTROCHEMICAL EVALUATION OF STAINLESS STEELS IN ACIDIFIED SODIUM CHLORIDE SOLUTIONS

L.M. Calle and L.G. MacDowell
NASA
Mail Code YA-C2-T
Kennedy Space Center, FL 32899

R.D. Vinje
ASRC Aerospace
Mail Code ASRC-15
Kennedy Space Center, FL 32899

ABSTRACT

This paper presents the results of an investigation in which several 300-series stainless steels (SS): AISI S30403 SS (UNS S30403), AISI 316L SS (UNS S31603), and AISI 317L SS (UNS S31703), as well as highly-alloyed: SS 254-SMO (UNS S32154), AL-6XN (N08367) and AL29-4C (UNS S44735), were evaluated using DC electrochemical techniques in three different electrolyte solutions. The solutions consisted of neutral 3.55% NaCl, 3.55% NaCl in 0.1N HCl, and 3.55% NaCl in 1.0N HCl. These solutions were chosen to simulate environments that are less, similar, and more aggressive, respectively, than the conditions at the Space Shuttle launch pads. The electrochemical test results were compared to atmospheric exposure data and evaluated for their ability to predict the long-term corrosion performance of the subject alloys. The electrochemical measurements for the six alloys indicated that the higher-alloyed SS 254-SMO, AL29-4C, and AL-6XN exhibited significantly higher resistance to localized corrosion than the 300-series SS. There was a correlation between the corrosion performance of the alloys during a two-year atmospheric exposure and the corrosion rates calculated from electrochemical (polarization resistance) measurements.

Keywords: S30403 (UNS S30403), 316L (UNS S31603), 317L (UNS S31703), 254-SMO (UNS S32154), AL-6XN (N08367), AL29-4C (UNS S44735), stainless steel, acidic NaCl, DC electrochemical measurements, atmospheric exposure.

INTRODUCTION

Type S30403 stainless steel, (S30403 SS), tubing is used in various supply lines that service the Orbiter at the Kennedy Space Center, (KSC), launch pads in Florida (USA). The atmosphere at the launch site has a very high chloride content caused by the proximity of the Atlantic Ocean. During a

launch, the exhaust products from the fuel combustion reaction in the solid rocket boosters produces hydrochloric acid, (HCl). The acidic chloride environment is aggressive to most metals and causes severe pitting in some of the common stainless steel alloys. Type S30403 SS tubing is susceptible to pitting corrosion (Figure 1) that lead to cracking and rupture (Figure 2) of high-pressure gas and fluid systems.[1] Such failures can be life-threatening to launch pad personnel in the immediate vicinity.

Outages in the systems where failures occur can impact normal operation and shuttle launch schedules. The use of a better tubing alloy for launch pad applications would greatly reduce the probability of failure, improve safety, lessen maintenance costs, and reduce downtime. The objective of this work was to study the electrochemical behavior of several candidate corrosion-resistant tubing alloys to replace the existing S30403 SS tubing at the Space Shuttle launch sites. The stainless steel alloys chosen for this investigation were: S30403, S31603, S31703, N08367, S44735 and S32154. Type S30403 SS was included in the study as the control. These alloys were tested in three different electrolytes that provided less severe, similar, and more aggressive conditions, respectively, than those found at the launch pads at the Kennedy Space Center in Florida (USA).

MATERIALS AND METHODS

Samples

Table 1 lists the tubing alloys chosen for this investigation. Table 2 lists common name, UNS number, and chemical composition of each material. The specimens were flat sample coupons, 3.2 cm in diameter, supplied by Metal Samples Co. (Munford, AL). The test specimens were polished to 600-grit, ultrasonically degreased in a detergent solution, and wiped with acetone before testing.

TABLE 1
ALLOYS TESTED

Alloy	Class
S30403	Low carbon austenitic stainless steel
S31603	Molybdenum-containing austenitic stainless steel
S31703	Molybdenum-containing austenitic stainless steel
N08367	Superaustenitic stainless steel
S44735	Superferritic stainless steel
S32154	Superaustenitic stainless steel

Electrochemical Measurements

A model 352 SoftCorr™ III Corrosion Measurement System, by EG&G Princeton Applied Research, was used for all electrochemical measurements. The equipment included software designed to measure and analyze corrosion data. The electrochemical flat cell included a saturated calomel reference electrode, (SCE), a platinized niobium counter electrode, the test (working) electrode, and a bubbler/vent tube. The specimen holder in the cell is designed such that the exposed metal surface area is 1 cm^2.

Three different aerated electrolyte solutions were used: 3.55% NaCl, 3.55% NaCl in 0.1N HCl and 3.55% NaCl in 1.0N HCl. These solutions were intended to simulate less than, similar to, and more aggressive conditions, respectively, than those found at the launch pads at KSC.

Corrosion potential, linear polarization resistance and cyclic polarization measurements were made for the alloys under the three different electrolyte conditions. Polarization resistance determinations were generally based on ASTM G 59[2]. Cyclic polarization data were gathered using ASTM G 61[3] as a guideline. Duplicate and triplicate tests indicated good reproducibility of results. The reported results are the averages of two or more runs.

A potential range of ±20 mV versus open circuit potential was used for the linear polarization measurements. The scan rate was 0.166 mV/sec. A linear plot of potential (E) versus current (I) was obtained and the polarization resistance (R_p) calculated.

Cyclic polarization measurements were started at –250mV relative to the corrosion potential (E_{corr}). The scan rate was 0.166mV/sec. The scans were reversed when the current density reached 5mA/cm^2. The reverse scan was continued until the potential returned to the starting potential of –250 mV relative to E_{corr}. A graph of potential, (E), versus log current density, (log (I)), was obtained. From this graph, the breakdown potential (E_{bd}), repassivation potential (E_{rp}), and the area of the hysteresis loop were obtained. Linear and cyclic polarization results were calculated using the SoftCorr III software.

TABLE 2
CHEMICAL COMPOSITION OF STAINLESS STEELS ALLOYS

Alloy	S30403	S31603	S31703	N08367	S44735	S32154
Fe	71.567	69.053	63.525	48.118	66.594	55.162
Ni	8.200	10.140	13.200	23.88	0.260	17.900
Cr	18.33	16.240	18.100	20.470	28.750	20.000
Mo	0.500	2.070	3.160	6.260	3.780	6.050
Mn	1.470	1.780	1.510	0.300	0.260	0.490
C	0.023	0.019	0.017	0.020	0.020	0.012
N	0.030	0.050	0.030	0.330	0.031	0.196
Si	0.380	0.280	0.460	0.40	0.280	0.350
P	0.030	0.027	0.027	0.021	0.023	0.019
S	0.0002	0.001	0.001	0.0003	0.002	0.001
Cu	0.460	0.340	0.150	0.200		0.680
Co		0.240				
Nb					0.290	
Ti					0.360	

Atmospheric Exposure

A beach site (Figure 3) was used to evaluate the performance of the six alloys included for resistance to localized corrosion under atmospheric conditions similar to those at the launch pad. The site is located at approximately 1 mile (2 km) south from launch complex 39A and is approximately 100 feet (30 m) from the high tide line directly on the Atlantic Ocean. Three sample tubes of each alloy were exposed. A 10 percent (v/v) solution of HCl and 28.5 grams of alumina powder per 500 ml of solution was mixed into acid slurry to simulate deposition from solid rocket booster emission and fallout. One set of tubes was sprayed every two weeks with the acid slurry to accelerate the corrosion effect. The other set was left exposed to the natural marine seacoast environment. A pressure gauge was attached to the

top end of the tubing. A ball valve was attached to the lower end for tube pressurization/isolation. The tubing test samples were pressurized to check for perforations (Figure 4).

RESULTS AND DISCUSSION

Corrosion Potential

Corrosion potential gives a relative thermodynamic "ranking" of a metal or alloy in a given environment. In general, a more positive corrosion potential means that the metal can be expected to be more resistant to corrosion in that particular electrolyte than one with a more negative corrosion potential. However, renking corrosion resistance based on corrosion potential is not very reliable. Therefore, other methods are used to determine actual or likely corrosion behavior. Stainless steels can exhibit active or noble potentials depending on whether they incur corrosion or are in a passive state depending on the environment to and other factor.

The corrosion potential of each alloy was monitored from the initial time of immersion until a nearly stable potential was observed. The alloys differed in the time it took for the potential to stabilize. For simplicity, Figure 5 shows only the open circuit potential for the SS alloys at times just prior to and during stabilization. Table 3 lists the average value of the stable open circuit potential. Contrary to what was expected based on the composition of the alloys, the highly alloyed SS S32154, N08367 and S44735 did not exhibit a more noble stable potential compared to S31603 and S31703 in 3.55% NaCl (Figure 5a). This behavior did not correlate with the performance of the tubing samples exposed to the atmosphere at the corrosion test site. As expected, S30403 SS was the most active alloy in this environment with a stable corrosion potential of –173 mV vs. SCE.

In 3.55% NaCl in 0.1N HCl, the three highly-alloyed SS displayed more noble potentials than the 300-series SS, as expected based on compositions. This behavior became more pronounced when the concentration of HCl in the 3.55% NaCl solution was increased to 1.0N. Figure 5c shows a clear distinction between the more noble behavior of the highly-alloyed SS in the 3.55% NaCl in 1.0N HCl solution and the more active behavior of the 300-series SS. The ennoblement of the higher-alloyed SS, as the concentration of HCl, in the 3.55% NaCl solution increased, was most pronounced for S44735 (269 mV ennoblement of the corrosion potential) followed by N08367 (153 mV noble shift) and S32154 (144 mV noble shift).

Qualitatively, this behavior correlated very well with the actual corrosion performance of the alloys under atmospheric exposure. The transition toward a more active corrosion potential of the 300-series SS as the concentration of HCl in the electrolyte increased can be attributed to the fact that these SS are easily attacked by HCl because the passive film is more easily damaged and less likely to repassivate.[4] Chloride (Cl^-) ions are well known for their ability to attack SS by penetrating the protective layer at any discontinuity of the oxide film. The addition of HCl, a reducing acid, exacerbates the attack by interfering with the formation of the oxide film.[5]

Polarization Resistance

Figure 6 shows linear polarization plots for S31603 SS in 3.55% NaCl with increasing HCl concentrations (neutral (a), 0.1N (b), and 1.0N (c)). It is evident from the figure that the slope of the line decreases as the acidity of the 3.55% NaCl solution increases. This behavior is indicative of decrease in the polarization resistance. Table 4 summarizes the polarization resistance, R_p, values in neutral 3.55% NaCl, 3.55% NaCl in 0.1N HCl, and in 3.55% NaCl in 1.0N HCl for all the alloys. The R_p values show

that increasing the HCl concentration in the 3.55% NaCl solution resulted in a significant decrease in the R_p values of the 300-series SS. The decrease in the R_p values, indicative of an increase in the corrosion rate, with increasing concentration of HCl, can be attributed to the fact that the protective oxide layer of the 300-series SS becomes unstable. This is illustrated by the drastic decrease in R_p from 1.36 Mohms.cm^2 in neutral 3.55% NaCl to 159 ohms.cm^2 in 3.55%NaCl in 1.0N HCl for S31603 SS (Figure 6 and Table 4).

R_p values for N08367, S44735, and S32154 in neutral 3.55% NaCl were approximately of the same order of magnitude as those for the 300-series SS. However, the R_p values for these alloys remained high as the concentration of HCl in the 3.55% NaCl solution increased. N08367 and S32154 showed a slight decrease in R_p as the concentration of HCl increased while S44735 exhibited no change in Rp after the initial slight increase. The lower corrosion rates of N08367, S44735, and S32154 SS can be attributed to the presence of greater amounts of chromium, nickel and molybdenum that result in a more stable protective oxide layer on the surface of the alloy. The low corrosion rate of S44735, which remained fairly unchanged with increasing concentration of HCl, can be attributed to its high (28.750%) chromium content.

Cyclic Polarization

Cyclic Polarization measurements were performed in order to determine the tendency of the alloys to undergo localized (pitting or crevice) corrosion when placed in the electrolyte solutions. A plot of potential versus log of the current density reveals the tendency of the material to undergo localized attack. Differences between the forward and reverse scans result in hysteresis loops. If the hysteresis loop is positive (i.e. the current density during the reverse scan is higher than that for the forward scan at any given potential), the area under the loop indicates the amount of localized corrosion incurred by the material. No hysteresis or a "negative loop (i.e. the current density during the reverse scan is lower than that for the forward scan at any given potential) indicates high resistance to localized corrosion. In the present case, the forward and reverse scans overlap almost exactly.[6,7]

Two important potentials, also used to characterize the hysteresis loop, are the critical breakdown potential, (E_{bd}), defined as the potential "knee" in the forward scan. Pitting is characterized by a rapid increase in current with a very small change in potential. Above this potential, pits initiate and propagate. The repassivation potential, (E_{rp}), is defined as the point where the reverse scan intersects the forward scan. At this potential, localized attack stops and the current decreases significantly. The more positive the value of E_{bd}, the more resistant the alloy is to initiation of localized corrosion. Also, the more positive the value of E_{rp}, the higher the corrosion resistance.[8] Values of E_{bd} and E_{rp} for the SS alloys in the three different electrolytes are shown in Table 5.

TABLE 3
CORROSION POTENTIALS OF SS ALLOYS

Alloy	E_{corr} (mV)		
	Neutral	0.1N HCl	1.0N HCl
S30403	-155	-122	-349
S31603	-102	-130	-320
S31703	-111	-150	-318
N08367	-125	12	28
S44735	-132	110	137
S32154	-132	-48	12

Hysteresis loop areas for all the SS alloys included in this investigation are given in Table 6. Alloy S44735 is very resistiant to localized corrosion as indicated by the very small hysteresis loop area obtained in neutral 3.55% NaCl. The increase in the acid concentration of the 3.55% NaCl solution to 0.1N resulted in a "negative" hysteresis loop. A further increase to 1.0N in the concentration of the acid did not produce any hysteresis. Alloys N08367 and S32154 exhibited small hysteresis loops in the three electrolytes indicating high resistance to localized corrosion in neutral and acidified 3.55% NaCl.

TABLE 4
POLARIZATION RESISTANCE OF SS ALLOYS IN 3.55% NACL IN VARIOUS CONCENTRATIONS OF HCL

Alloy	R_p (ohms.cm^2)		
	Neutral	**0.1N HCl**	**1.0N HCl**
S30403	6.37×10^5	7.05×10^5	2.00×10^2
S31603	1.36×10^6	4.80×10^5	1.59×10^2
S31703	1.49×10^6	2.99×10^5	1.93×10^2
N08367	1.40×10^6	1.18×10^6	0.615×10^6
S44735	0.882×10^6	1.09×10^6	1.09×10^6
S32154	1.08×10^6	1.01×10^6	0.782×10^6

TABLE 5
CRITICAL BREAKDOWN AND REPASSIVATION POTENTIALS FOR SS ALLOYS IN 3.55% NACL IN VARIOUS CONCENTRATIONS OF HCL

Alloy	Neutral		0.1N HCl		1.0N HCl	
	E_{bd} (mV)	E_{rp} (mV)	E_{bd} (mV)	E_{rp} (mV)	E_{bd} (mV)	E_{rp} (mV)
S30403	366	-136	167	-153	-60	-58
S31603	380	-143	135	-164	-42	-37
S31703	622	-131	432	-91	-90	-89
N08367	922	906	816	835	902	904
S44735	964	964	818	N/A	878	N/A
S32154	952	939	825	831	877	890

Cyclic polarization scans for three of the alloys are shown in Figures 7-9. Figure 7 shows a cyclic polarization scan for alloy S44735 in 3.55% NaCl-1.0N HCl. In this case, the reverse scan followed the forward scan almost exactly resulting in no hysteresis. This is characteristic of an alloy that is highly resistant to localized corrosion. Figure 8 shows the overlay of the cyclic polarization scans for S31603 SS and S32154 SS in 3.55% NaCl-1.0N HCl. The hysteresis loop area values for these two alloys are very similar under these conditions (5.58 and 5.98 coulombs respectively) suggesting high resistance to localized corrosion. However, the values of E_{bd} and E_{rp} relative to E_{corr} are also very important when analyzing cyclic polarization data. While the area of the hysteresis loop is very similar, (Figure 8), E_{bd} and E_{rp} values for S31603 SS are –42 mV and –37 mV, respectively, while the values for S32154 are 877 mV and 890 mV, respectively. These results indicate that S32154 has superior corrosion resistance to localized corrosion than S31603 SS under the same conditions. Results for N08367 and S44735 were similar to those obtained for S32154.

Figure 9 shows the effect of increasing HCl concentration on the cyclic polarization curves for S30403 SS. The scan in neutral 3.55% NaCl solution displays a more noble corrosion potential as well as lower current density. When the HCl concentration was increased to 0.1N, the corrosion potential

became more negative and the current density increased. The metal still portrays passive behavior where the voltage increases with small changes in current density. However, increasing the acid concentration to1.0N HCl affects the alloy more drastically. At potentials more noble than E_{corr}, S30403 SS experiences anodic dissolution and then repassivates over a small voltage range and rapidly experiences breakdown of the passive film at E_{bd}. Similar behavior was observed for the other 300-series SS. For these alloys, a decrease in the hysteresis loop area cannot be interpreted as an indication of increased resistance to localized corrosion.

A decrease in the difference between E_{corr} and E_{bd} has been associated with increased susceptibility to localized corrosion.[9] Table 7 shows the values for the difference between E_{corr} and E_{bd} for the SS alloys in the three different electrolytes. The values for the 300-series SS are lower than those for the higher-alloyed materials. The difference decreases as the concentration of acid in the electrolyte increases; this effect is greater for the 300-series SS than for the higher-alloyed materials. These results are in agreement with those from visual observations as well as the atmospheric exposure of the samples.

TABLE 6
AREAS OF HYSTERESIS LOOPS FOR SS ALLOYS IN 3.55% NACL WITH VARIOUS CONCENTRATIONS OF HCL

	Area of Hysteresis Loop (Coulombs)		
Alloy	**Neutral**	**0.1N HCl**	**1.0N HCl**
S30403	22.96	11.36	10.42
S31603	15.99	12.35	5.58
S31703	33.12	23.53	12.58
N08367	5.07	3.23	1.69
S44735	5.23	Negative Hysteresis	No Hysteresis
S32154	5.11	4.85	5.98

Visual observation of the samples at the conclusion of the cyclic polarization measurements revealed that the 300-series SS samples experienced crevice corrosion in all three electrolytes. Alloys S32154, N08367 and S44735 experienced some crevice corrosion but only under neutral conditions. This can be attributed to the fact that the interface between the metal coupon and the cell gasket creates a site favorable for crevice corrosion. The areas of the hysteresis loops from the cyclic polarization scans account for both pitting and crevice corrosion whenever they are present. Breakdown or pitting potential as well as repassivation potential also correspond well with the crevice corrosion observed. The potential for initiation of crevice corrosion is more active than E_{pit} for the same alloy, because of the favorable geometric conditions for deaeration and chloride concentration.[10]

Pitting Resistance Equivalent Number

It is often stated that the pitting corrosion resistance of stainless steels depends mainly upon the chromium, molybdenum, and nitrogen content. One method of estimating the pitting resistance equivalent number (PREN) is as follows:

$$PREN = (\%Cr) + 3 \times (\%Mo) + 15 \times (\%N)$$

where the percentage corresponds to the weight percentage of Cr, Mo, and N in the alloy.[11-13] PREN numbers for the alloys investigated are shown in Table 8. The alloy rankings according to PREN are in good agreement with the experimental results of this investigation.

TABLE 7
DIFFERENCE BETWEEN E_{corr} AND E_{bd} FOR SS ALLOYS IN 3.55% NACL WITH VARIOUS CONCENTRATIONS OF HCL

Alloy	E_{bd}-E_{corr} (mV)		
	Neutral	0.1N HCl	1.0N HCl
S30403	514	401	287
S31603	510	424	271
S31703	810	730	221
N08367	1081	895	950
S44735	1129	757	746
S32154	1106	978	944

TABLE 8
PREN NUMBERS FOR STAINLESS STEEL ALLOYS

Alloy	S30403	S31603	S31703	N08367	S44735	S32154
PREN	19	26	31	46	40	43

Atmospheric Exposure

The most important validation of any laboratory test for localized corrosion is that results must correlate with alloy performance in service environments. In this study, the laboratory results were compared to two-year atmospheric exposure data. Detailed results of the atmospheric exposure have been previously reported elsewhere.[14] Photographs of the tubes after one-year of atmospheric exposure with no acid rinse are shown in Figure 10. Photographs of the tubes after two years of atmospheric exposure with biweekly acid rinse are shown in Figure 11. A photograph of S30403 SS is not shown because the tube failed prior to the two-year evaluation and was removed from the test rack. A summary of the visual evaluation of the tubing test articles after two years of atmospheric exposure is shown in Table 9.

CONCLUSIONS

Electrochemical measurements of the six alloys indicated that the higher-alloyed S32154, S44735, and N08367 SS exhibited significantly higher resistance to localized corrosion than the 300-series SS.

The stable corrosion potential values obtained in neutral 3.55% NaCl did not correlate with the performance of the alloys under natural seacoast atmospheric exposure.

A correlation was found between the stable corrosion potential values obtained in acidified 3.55% NaCl and the corrosion performance of the alloys under atmospheric exposure with and without acid rinse.

There was a correlation between the corrosion performance of the alloys during the two-year atmospheric exposure and the corrosion rates based on polarization resistance values.

The area of the hysteresis loop in a cyclic polarization curve cannot be used as the sole criterion to predict susceptibility to localized corrosion.

There was a correlation between the atmospheric exposure data and the susceptibility to localized corrosion that was predicted based on the difference between E_{bd} and E_{corr}. These predictions were in agreement with the expectations based on the PREN calculated for the alloys.

TABLE 9
VISUAL OBSERVATIONS OF TUBE SPECIMENS AFTER TWO YEARS OF ATMOSPHERIC EXPOSURE

Visual Observations after Two Years of Atmospheric Exposure		
Alloy	**Natural**	**With Acid-Alumina Slurry Rinse**
S30403	Tubes in poor condition with pits and brown spots all over	Tubes failed due to pitting. Pits went through the thickness of the tube
S31603	Tubes in poor condition with pits and brown stains. Better than S30403	2 out of 3 tubes failed. Remaining tube in bad condition with brown spots and pits all over
S31703	Brown spots and pits on the tube. Better than S31603	1 out of 3 tubes failed. Pits and brown spots all over the tube. Better condition than S31603
N08367	Light browning of the tube.	Tubes look in good condition with slight discoloration
S44735	Slight discoloration of the tubes. Overall in good condition.	Tubes in good condition
S32154	Tube is in good condition. Some spots along the seam weld	Tubes look very good except for pits on the seam weld

REFERENCES

1 S.J. McDanels, Failure Analysis of Launch Pad Tubing, Microstructural Science, **25**, p. 125-129 (1998).

2 ASTM G 59 – 97 (Reapproved 2003), "Standard Test Method for Conducting Potentiodynamic Polarization Resistance Measurements" (West Conshohocken, PA: ASTM International, 2003).

3 ASTM G 61 – 86 (Reapproved 2003), "Standard Test Method for Conducting Cyclic Potentiodynamic Measurements for Localized Corrosion Susceptibility of Iron-, Nickel-, or Cobalt-Based Alloys" (West Conshohocken, PA: ASTM International, 2003).

4 Metals Handbook, Vol. 13, p. 557, (ASM International, Metals Park, OH, 1987).

5 N.G. Thompson and J.H. Payer, DC electrochemical Test Methods, p. 57, (Houston, TX: NACE International, 1986).

6 W.S. Tait, Corrosion, 34 (6) (1978): pp.214-217.

7 W.S. Tait, corrosion, 35 (7) (1979): pp. 296-300.

8 Z. Szklarska-Smialowska, M. Janik-Czacho, Corros. Sci. 11 12(1971): p. 901.

9 J. Beddoes and J. Gordon Parr, Introduction to Stainless Steels (ASM International, Materials Park, OH), 1999, p. 83.

10 D.A. Jones, Principles and Prevention of Corrosion (Prentice Hall, Upper Saddle River, NJ), Second Edition, 1996, p. 223,

11 M.J. Matthews, Metall. Mater. Technol. 5 (1982): p. 205.

12 C.A. Clark, P. Gentil, P. Guha, "Development of Improved Alloy Duplex Steel, ed. J. Van Liere (The Hague, The Netherlands: Netherlands instituut Voor Lastechniek, 1986).

13 A.J. Sedriks, Corrosion, Vol. 42, 7 (1986): p. 376.

14 R.G. Barile, L.G. MacDowell, J. Curran, L.M. Calle, and T. Hodge, "Corrosion of Stainless Steel tubing in a Spacecraft Launch Environment," Paper No. 02152, Corrosion/2002, 57th Annual Conference & Exposition, April 7-11, 2002, Denver, Colorado.

FIGURE 1. Micrograph (100x magnification) of pit from KSC's launch pad S30403 SS tubing.

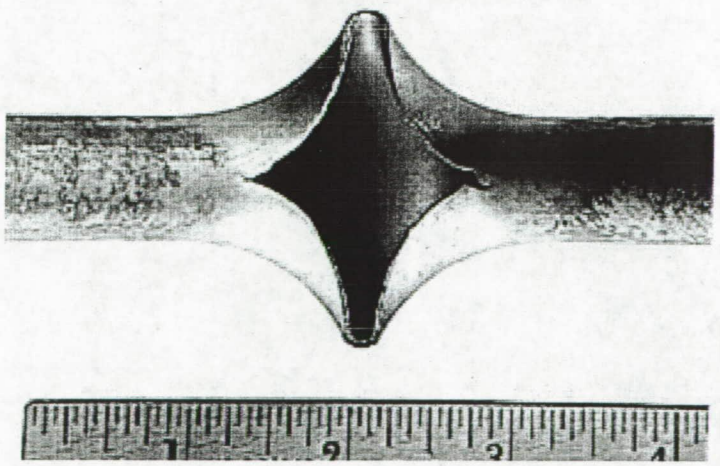

FIGURE 2. Tubing split caused by pitting.

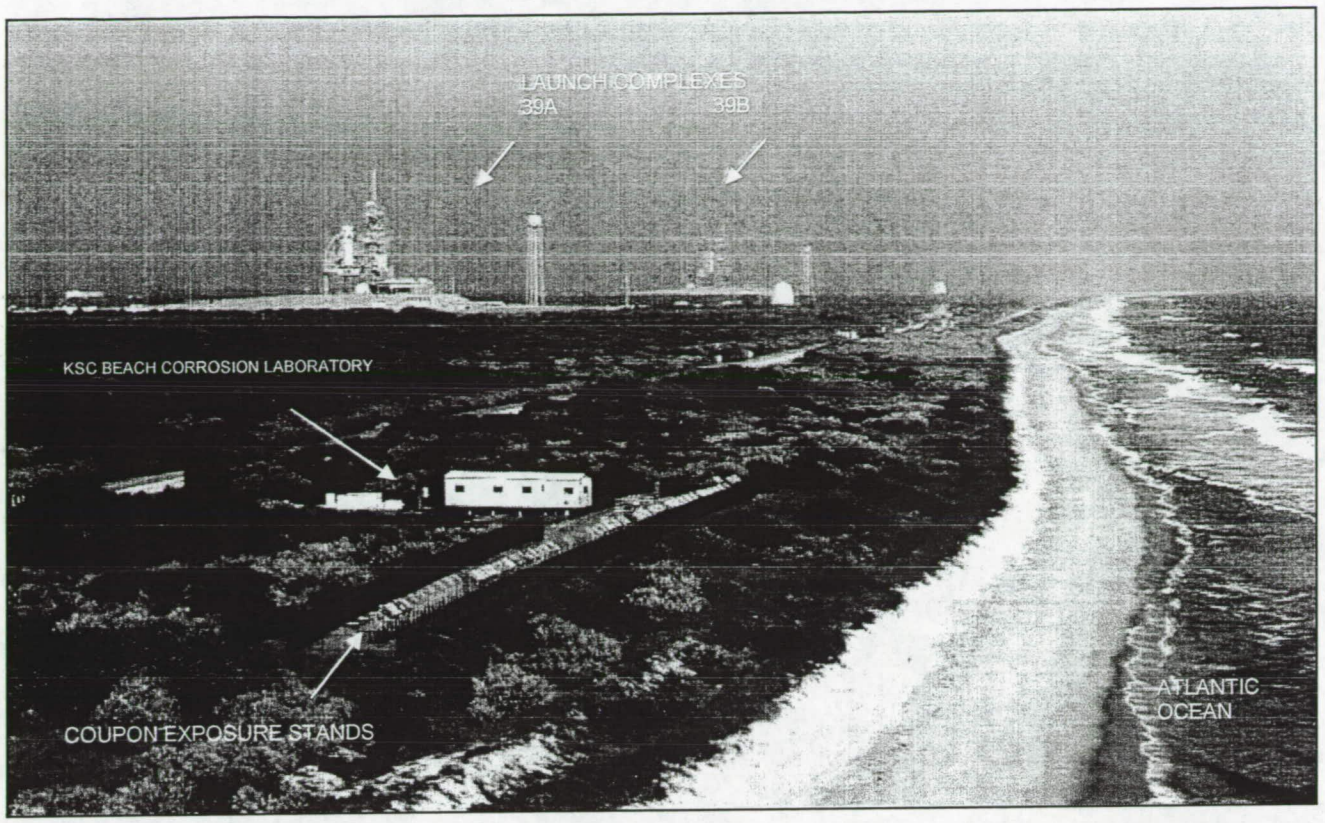

FIGURE 3. KCS's Beach Corrosion Test Site. Photo courtesy of NASA.

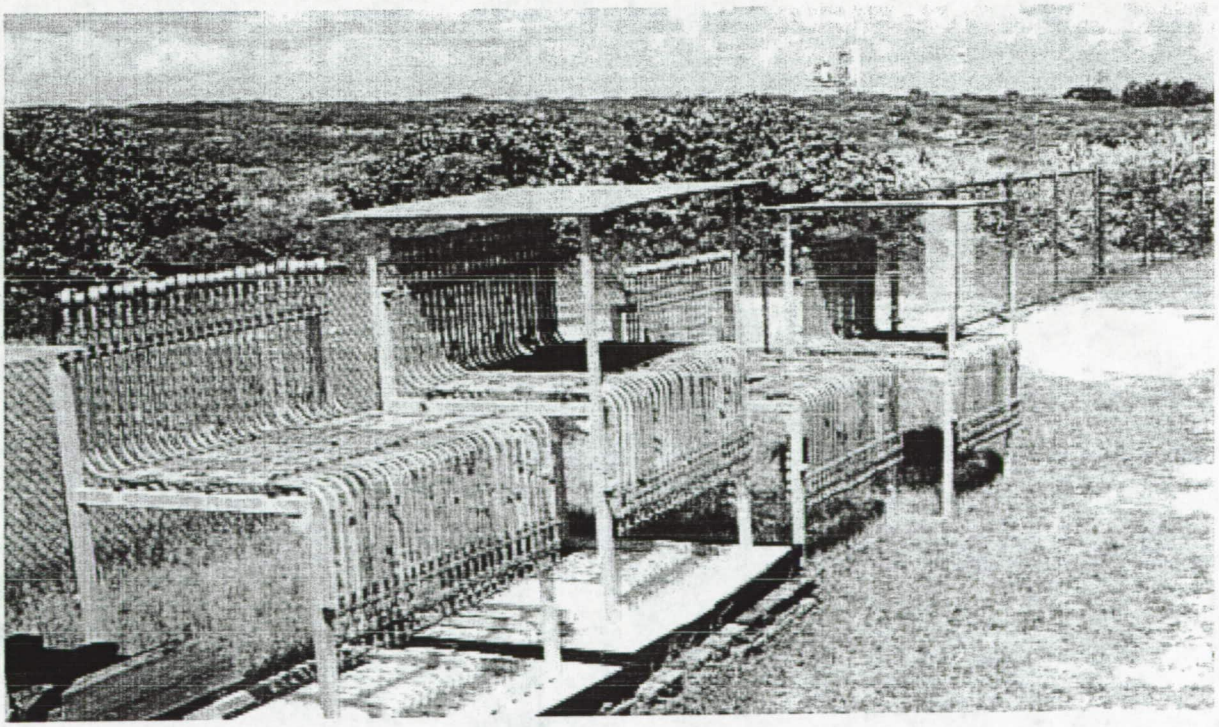

FIGURE 4. Tube Samples on Test Racks at KSC's Beach Corrosion Test Site

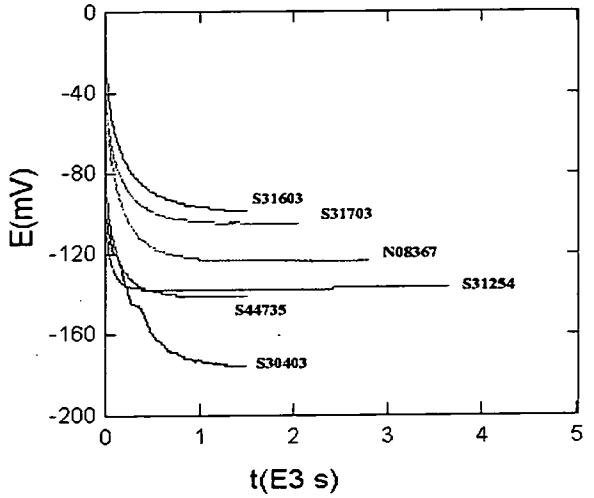

(a)

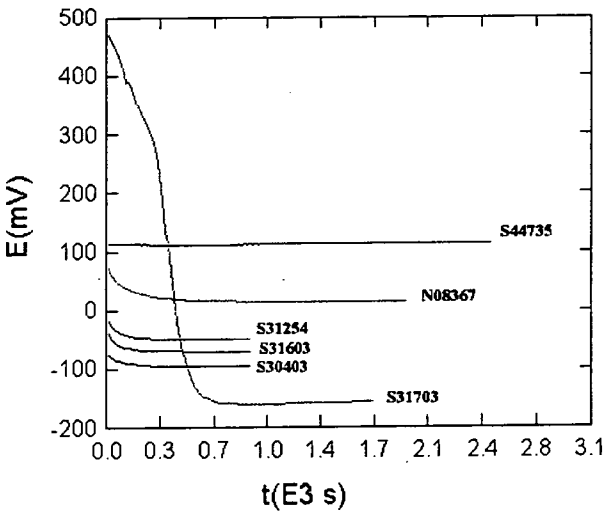

(b)

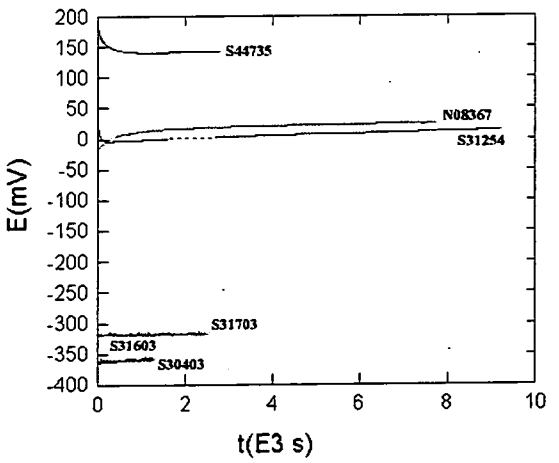

(c)

FIGURE 5. Corrosion potential of SS Alloys in (a) neutral 3.55% NaCl, (b) 3.55% NaCl-0.1N HCl, and (c) 3.55% NaCl-1.0N HCl.

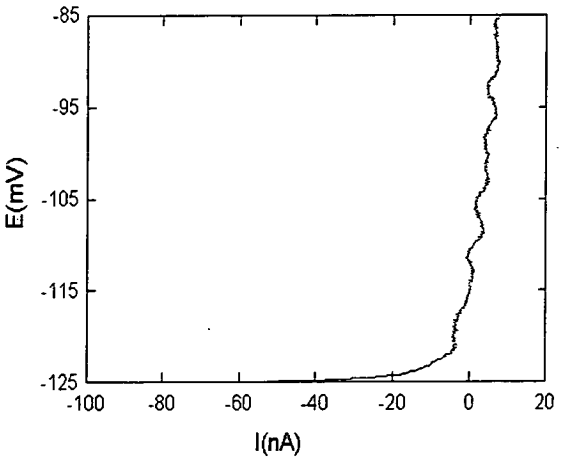

(a)

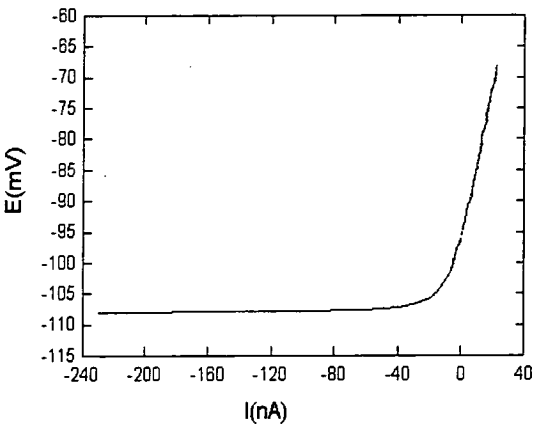

(b)

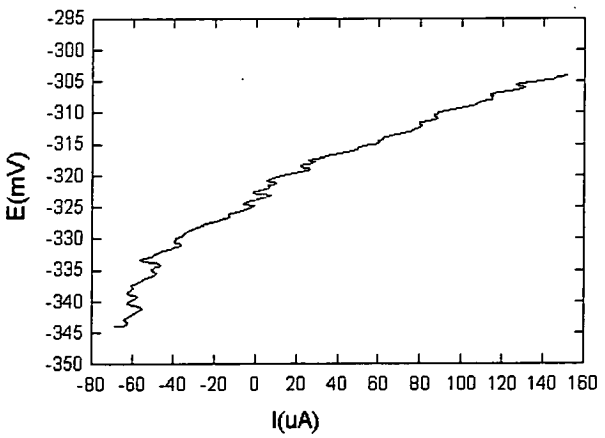

(c)

FIGURE 6. Linear polarization curves for S31603 in (a) neutral 3.55% NaCl, (b) 3.55% NaCl-0.1N HCl, and (c) 3.55% NaCl-1.0N HCl

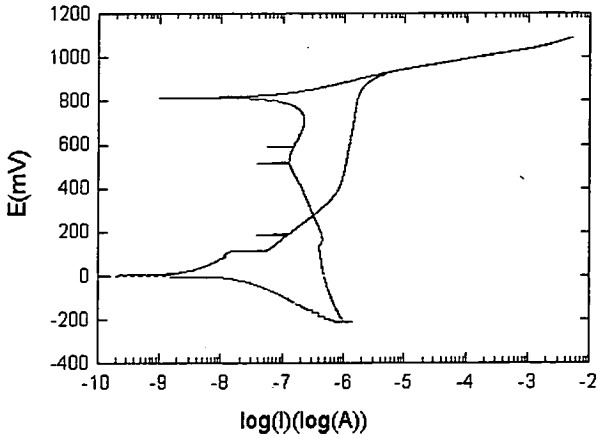

FIGURE 7. Cyclic polarization curve for S44735 in 3.55% NaCl-1.0N HCl

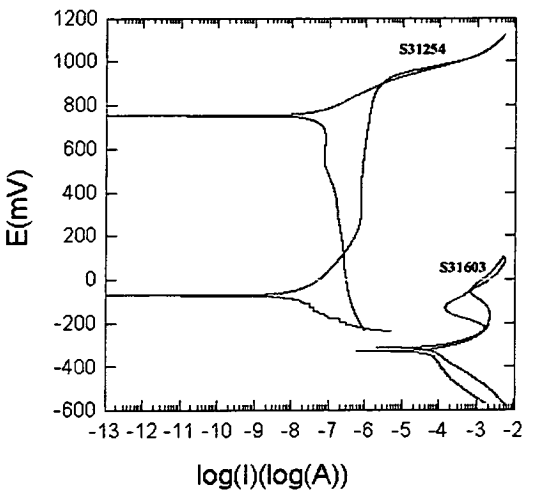

FIGURE 8. Cyclic polarization curves for S31603 SS and S32154 in 1.0N-HCl 3.55% NaCl

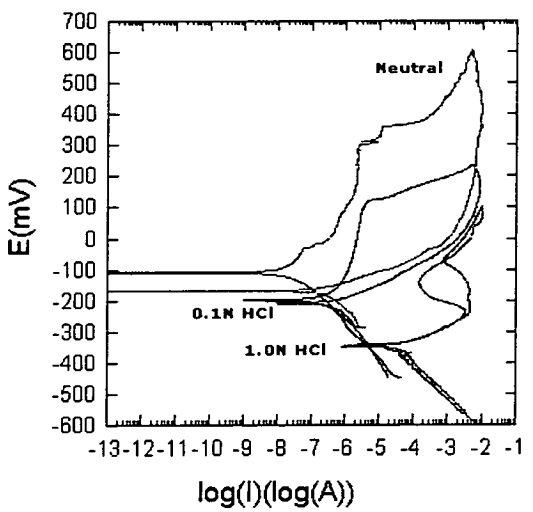

FIGURE 9. Cyclic polarization curves for S30403 SS in neutral, 0.1N and 1.0N HCl-3.55% NaCl solutions

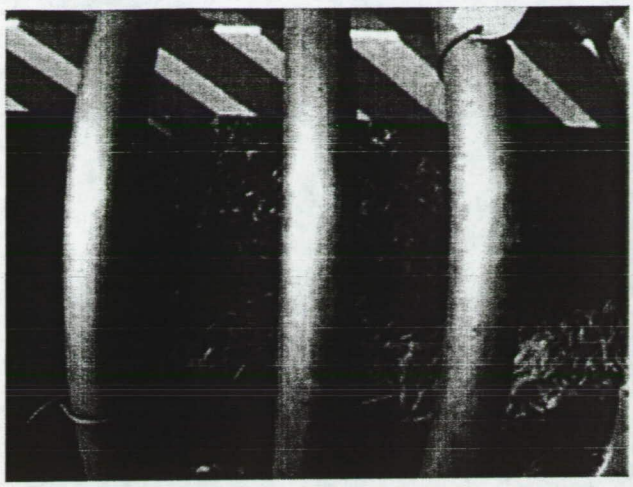

S30403

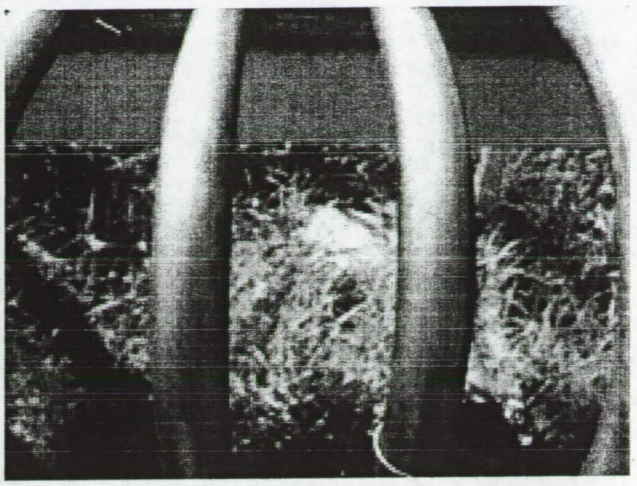

S31603

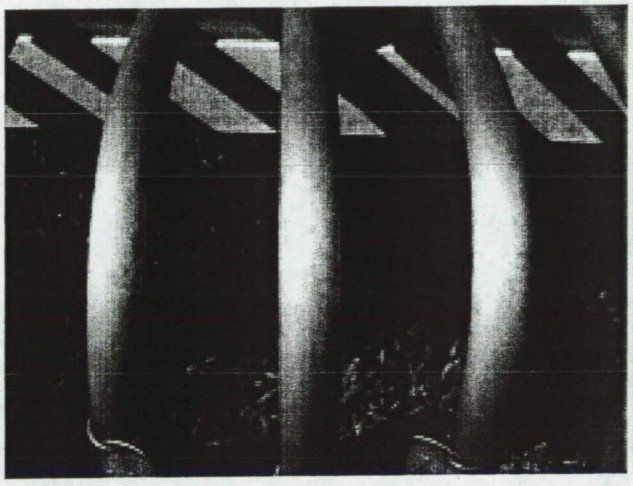

S31703

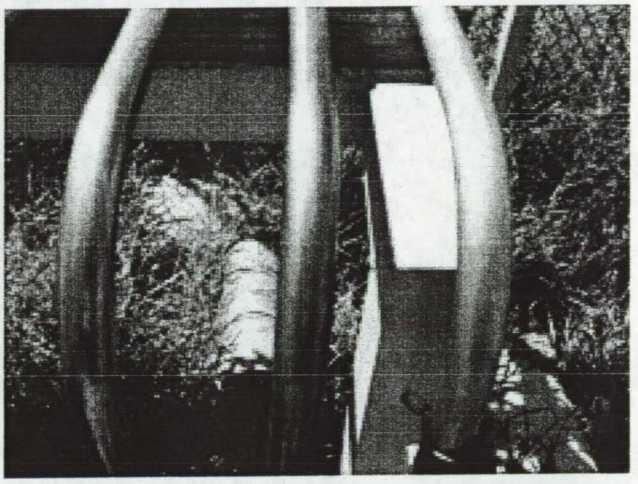

S44735

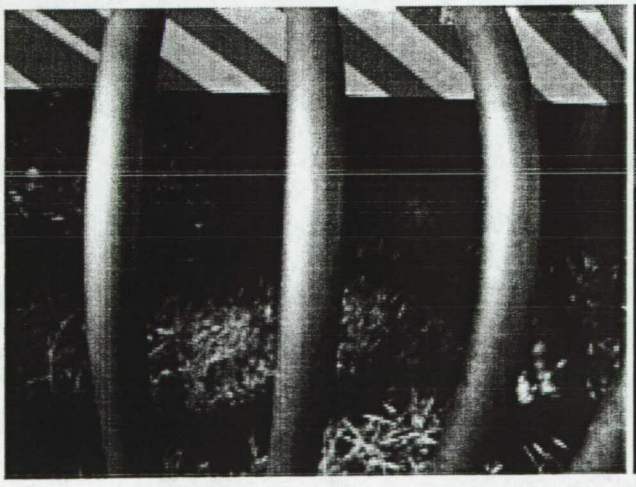

N08367

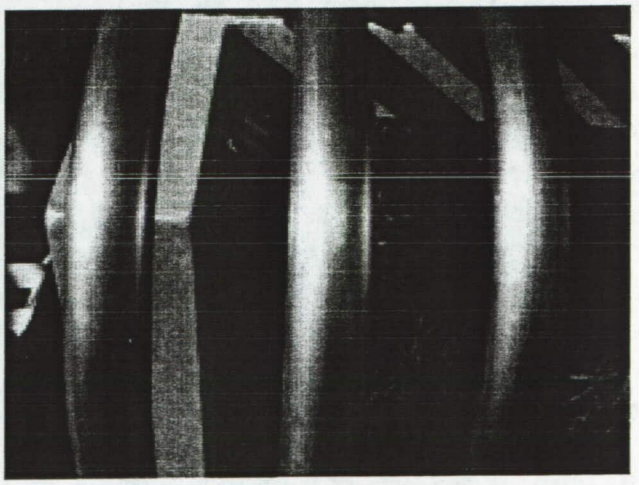

S31254

FIGURE 10. Tubing after one year of natural seacoast atmospheric exposure (no acid rinse).

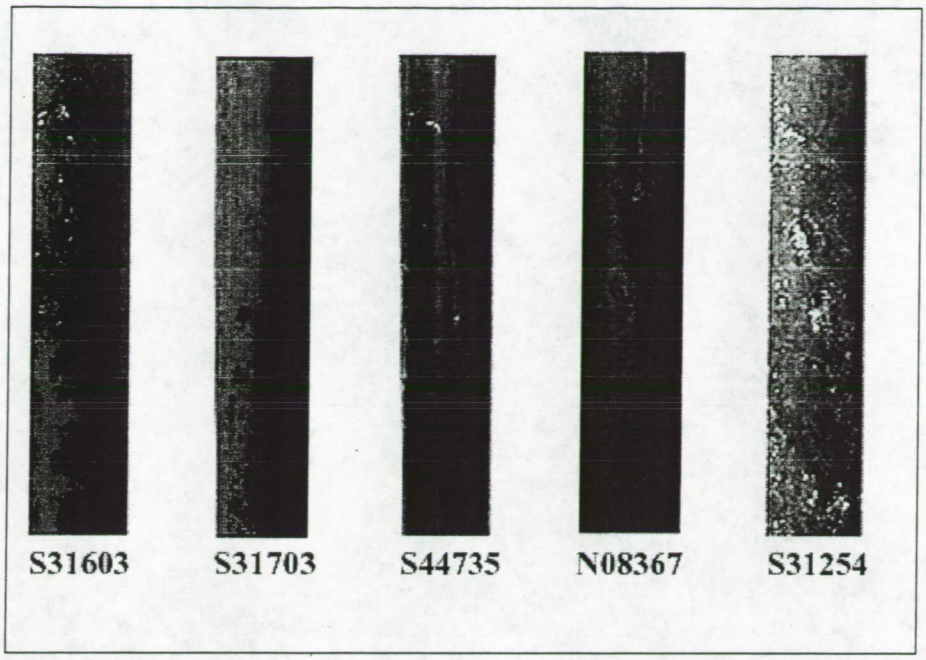

FIGURE 11. Photographs of tubing sections after two years of seacoast atmospheric exposure with acid rinse every two weeks